Effect of DNA Polymerase β Loop Variants on Discrimination of O^6-Methyldeoxyguanosine Modification Present in the Nucleotide versus Template Substrate†

Subarna Hamid and Kristin A. Eckert*

Department of Biochemistry and Molecular Biology, The Gittlen Cancer Research Institute, and MD-PhD Program, Pennsylvania State University College of Medicine, 500 University Drive, Hershey, Pennsylvania 17033

Received December 6, 2004; Revised Manuscript Received April 15, 2005

ABSTRACT: We have examined the mechanism of DNA polymerase β (pol β) lesion discrimination using alkylated dNTP versus alkylated DNA template substrates and the pol β variants R253M and E249K. Both of these amino acid variants are located in the loop region of the palm domain and are known to play a role in pol β fidelity and discrimination of 3′-azido-3′-deoxythymidine triphosphate substrates. We observed that these variants affect O^6-methyldeoxyguanosine- (m6G-) modified dNTP discrimination without affecting m6G template translesion synthesis. Under steady-state conditions, the ratio of inherent reactivity values for the m6dGTP substrate relative to the dGTP substrate was greater for both variant polymerases than for wild-type (WT) pol β. Biochemical assays of translesion synthesis using m6G lesion-containing templates demonstrated no significant differences between the variants and WT. Using *N*-methyl-*N*-nitrosourea- (MNU-) modified DNA templates in the HSV-*tk* in vitro assay, no difference among the enzymes in the frequency of alkylation-induced G to A transition mutations was observed. However, differences among the polymerases in the frequency of alkylation-induced C to A transversions were observed, consistent with a mutator tendency for E249K and an antimutator tendency for R253M. We conclude that a specific interaction at the loop of the palm domain is involved in pol β discrimination of the m6G lesion when present on the incoming dNTP substrate but not when present in the DNA template. Our data support a role for the flexible loop in pol β error discrimination.

DNA polymerase β (pol β)[1] is a 39 kDa nuclear polymerase actively involved in base excision repair (BER) (*1*) and implicated in the process of meiotic recombination (*2*). Pol β is a key player in the repair of DNA damage induced by anticancer agents such as bleomycin, γ-irradiation, and alkylating agents (*3*, *4*). Mechanistic studies of pol β are important for understanding its diverse roles in DNA metabolism under circumstances leading to mutagenesis, cytotoxicity, and the resistance of tumors to anticancer therapy. The mechanistic determinants of pol β fidelity have been examined, both structurally and kinetically (reviewed in ref *5*). The small size, single subunit composition, and availability of physical structures make pol β a good model for structure−function studies. Pol β residues Arg-253 and Glu-249 are located in a disordered loop region of the palm domain of the enzyme (*6*, *7*). A role for the loop region of the palm in dNTP discrimination was first identified using an in vivo genetic screen for 3′-azido-3′-deoxythymidine triphosphate- (AZT-) resistant pol β variants (*6*). Pol β variant R253M exhibits a 2−3-fold increased discrimination in vitro when incorporating TTP vs AZT-TP, a nucleotide modified at the sugar moiety (sugar-modified dNTP). Pol β variant E249K, on the other hand, exhibits an altered kinetic mechanism of dNTP discrimination and displays an increased ability to extend template·dNTP mispairs (*7*). Therefore, both variants R253M and E249K have an altered ability to discriminate sugar-modified dNTPs compared to wild-type (WT) pol β and are located in the same region of the polymerase, away from the active site. However, R253M shows increased discrimination while E249K shows decreased discrimination of sugar-modified dNTPs (*6*, *7*). Several explanations have been proposed for how the loop domain variants affect nucleotide discrimination. Possibly, the loop may directly influence channeling of the dNTP substrate into the active site (*7*). Alternatively, as a structural part of the palm subdomain, the loop may act to maintain optimal active site geometry. Detailed kinetic analyses of a third variant in the loop region, D246V, provide experimental evidence that the flexible loop may function indirectly in nucleotide discrimination by modulating the DNA primer position within the pol β active site (*8*).

Our study was designed to determine if the characteristics of the pol β variants R253M and E249K extend to discrimination of dNTPs modified at the base moiety (base-modified dNTP) and base-modified template residues. Geometric selection for Watson−Crick (W/C) base pairs over mispairs by steric exclusion within the active site is hypothesized to play a major role in DNA polymerase fidelity (*9*). As such,

† This research was supported by American Cancer Society Grant RPG-95-075 and by generous donations to the Jake Gittlen Memorial Cancer Research Fund.

* To whom correspondence should be sent. Phone: 717-531-4065. Fax: 717-531-5634. E-mail: kae4@psu.edu.

[1] Abbreviations: AZT, 3′-azido-3′-deoxythymidine; pol β, DNA polymerase β; dNTP, deoxynucleoside 5′-triphosphate; m6G, O^6-methyldeoxyguanosine; HSV-*tk*, herpes simplex virus type 1−*thymidine kinase*; MNU, *N*-methyl-*N*-nitrosourea; TLS, translesion synthesis.

10.1021/bi047444i CCC: $30.25
Published on Web 07/07/2005

discrimination would be predominantly dependent on the overall shape of a purine−pyrimidine pair, with the precise specificity resulting from the complementary nature of the base pairing (*10*, *11*). The physical structures of base mispairs within the thermostable *Bacillus* DNA polymerase I active site have been solved (*12*). In these structures, some base pair parameters, such as the C1′−C1′ distance and bond angles of the complementary G·T and T·G wobble mispairs are similar to each other but distinct from W/C base pair angles. If pol β residues Arg-253 and Glu-249 contribute to dNTP discrimination by affecting recognition of the template·dNTP base pair geometry, we hypothesized that the R253M and E249K variant polymerases may recognize modified dNTPs and modified template residues to a similar extent due to similar geometric distortions in both cases. On the other hand, if Arg-253 and Glu-249 function to channel the dNTP or position the primer, we would expect that the variants would display differences between complementary mispairs.

To experimentally probe this hypothesis, we concentrated on the highly mutagenic and widely studied O^6-methyldeoxyguanosine (m6G) modification. Template m6G lesions have been observed to mispair with thymine both in vivo and in vitro, despite the slightly increased stability observed for the m6G·C base pairs relative to the m6G·T (reviewed in ref *13*). X-ray crystallographic and NMR data have demonstrated that the m6G·T base pair assumes a Watson−Crick-like conformation while the m6G·C base pair is in a wobble conformation, unless protonated, suggesting that base pair structure plays a role in m6G mutagenesis (*13*). Two conformers of the exocyclic O^6-methyl group relative to the N1 guanine position also have been described, which may act sterically to favor formation of certain base mispairs during DNA synthesis (*14*). The slow rate of dCMP incorporation opposite m6G by the Klenow fragment of *Escherichia coli* DNA polymerase I has been proposed to result from the unfavorable alignment of 3′OH for in-line attack of the incoming dNTP due to altered structure of the lesion base pair (*15*). Pol β was observed to incorporate TTP opposite m6G more efficiently than dCTP, while pol β extension synthesis from the nonmutagenic, wobble m6G·C substrate was favored over extension from the m6G·T substrate (*16*, *17*). On the other hand, the Klenow fragment of *E. coli* DNA polymerase I was observed to extend an m6G·T substrate more efficiently than an m6G·C substrate (*18*). Kinetic studies using m6G base analogues have provided evidence for hydrogen bond interactions between the Klenow polymerase and the N3 position of guanine during insertion of TMP but not dCMP opposite m6G (*19*). Biochemical analyses of the Klenow polymerase variants R668A and Q849A lacking primer or template strand interactions, respectively, demonstrated that interactions of the protein with the DNA minor groove are critical for maintaining the DNA−polymerase complex during m6G translesion synthesis (TLS) (*20*). The precise positions of hydrogen bonds between the enzyme and the DNA primer-template in the minor groove are different for DNA polymerase I family members and pol β (*21*, *22*). Altered contacts with the primer terminus might explain the lack of selectivity against the wobble geometry of the m6G·C terminal base pair by pol β, relative to the Klenow polymerase.

In this study we report that pol β variants R253M and E249K affect m6GTP discrimination without affecting m6G-template translesion synthesis and mutagenesis. Our study emphasizes the importance of the loop region in the palm domain for incoming nucleotide discrimination of pol β.

MATERIALS AND METHODS

Reagents. Wild-type and variant pol β vector clones were a gift from Dr. Joann Sweasy (Yale University). Recombinant rat DNA polymerase β wild type (WT), R253M, and E249K were purified from *E. coli* as described previously (*23*). *N*-Methyl-*N*-nitrosourea (MNU) was purchased from Sigma Chemical Co. (St. Louis, MO). O^6-Methyl-2′-deoxyguanine 5′-triphosphate (m6dGTP) and AZT-TP were purchased from Trilink Biotechnologies (San Diego, CA). The m6dGTP purity was reported to be 97.0% by HPLC and >95% by ^{31}P NMR by the manufacturer. rCTP was purchased from Amresco (Solon, OH).

Construction of Gapped DNA Templates. Oligonucleotides used in the construction of gapped templates are as listed in Figure 1. Gel-purified oligonucleotides corresponding to the HSV-*tk* genome sequence were purchased from Pierce (Rockland, IL) or Midland Certified Reagents Co. (Midland, TX). The site-specific m6G-containing oligonucleotide (m6G220) was purified via trityl-selective persion HPLC, and the presence of the lesion was confirmed by mass spectrometry by the manufacturer. Priming nucleotides were 5′-end-labeled with [γ-^{32}P]ATP (5000 Ci/mmol; Amersham Pharmacia) and T4 polynucleotide kinase (Gibco BRL). Downstream oligonucleotides were 5′ phosphorylated with T4 polynucleotide kinase and purified using 4 kD Eppendorf centrifugal filter tubes and G-25 Sephadex Quick Spin columns (Boehringer Mannheim). Gapped templates (5-nucleotide gap) were constructed by incubating both a priming and a downstream oligonucleotide with a template oligonucleotide in a 1:3:1 molar ratio, respectively, at 70 °C followed by cooling to room temperature. Hybridization reactions were purified with G-25 Sephadex Quick Spin columns.

Polymerase Insertion of Modified dNTP Substrates. Polymerase reactions were initiated by the addition of polymerase after preincubation of the reaction components at 37 °C for 3 min. Reactions were conducted at 37 °C using 1.5 pmol of primer-template in pol β reaction buffer [50 mM Tris-HCl, pH 8.5, 50 mM NaCl, 10 mM MgCl, 1 mM dithiothreitol, and 200 μg/mL bovine serum albumin (Gibco BRL)] and various nucleotide substrates. The concentrations of the three polymerases were adjusted for equivalent activity and steady-state excess substrate conditions. To assay for dGTP insertion opposite template C (Figure 1A), 0.10, 0.15, and 0.09 pmol of WT, R253M, and E249K pol β were used, respectively. To assay for m6dGTP insertion opposite template C (Figure 1A), 0.20, 0.3, and 0.18pmol of WT, R253M, and E249K pol β were used, respectively. To assay for dTTP insertion opposite template A (Figure 1D), 0.1 pmol of WT and 0.2 pmol of R253M were used ([dTTP] = 10−200 μM]. To assay for AZT-TP insertion opposite template A, 1 pmol of WT and 1 pmol of R253M were used ([AZT-TP] = 84−2000 μM). The assay for rCTP incorporation opposite template G used hybrid 9 (Figure 1E), 84−2000 μM rCTP, and 0.5 or 1 pmol of WT and R253M polymerase,

A. Insertion Assay with m6G-modified dNTP (Hybrid 1)

3′ GATGACGCCCAAATCTAG**C**AGCCAGGCGTCCCG 5′	Template (33mer)
5′ CTACTGCGGGTTTAGAT	Upstream (17mer)
GTCCGCACGGC 3′	Downstream (11mer)

B. Translesion Synthesis Assay, Insertion (Hybrids 2/3; G/m6G)

3′ CGGCACGCCTGGCT**G/m6G**CTAGATTTGGGCGTCATC 5′	Template (33mer)
5′ GCCGTGCGGACCG	Upstream (13mer)
CTAAACCCGCAGTAG 3′	Downstream (15mer)

C. Translesion Synthesis Assay, Extension

Hybrids 4/5 (G•C or m6G•C)

3′ CGGCACGCCTGGCT**G/m6G**CTAGATTTGGGCGTCATC 5′	Template (33mer)
5′ GCCGTGCGGACCGA**C**	Ex C Primer (15mer)
CTAAACCCGCAGTAG 3′	Downstream (15mer)

Hybrids 6/7 (G/m6G•T)

3′ CGGCACGCCTGGCT**G/m6G**CTAGATTTGGGCGTCATC 5′	Template (33mer)
5′ GCCGTGCGGACCGA**T**	Ex T Primer (15mer)
CTAAACCCGCAGTAG 3′	Downstream (15mer)

D. Insertion Assay with AZT-TP (Hybrid 8)

3′ GATGACGCCCAAATCT**A**GCAGCCAGGCGTGCCG 5′	Template (33mer)
5′ CTACTGCGGGTTTAGA	Primer (16mer)
GGTCCGCACGGC 3′	Downstream (12mer)

E. Insertion Assay with rCTP (Hybrid 9)

3′ GATGACGCCCAAATCTA**G**CAGCCAGGCGTGCCG 5′	Template (33mer)
5′ CTACTGCGGGTTTAGAT	Primer (17mer)
GTCCGCACGGC 3′	Downstream (11mer)

FIGURE 1: DNA primers and templates for the in vitro synthesis reactions. Sequences of templates are written 3′ to 5′ to show complementation with the primers and formation of the gapped substrates.

respectively. Reaction aliquots were quenched at various time points in equal volume stop dye. Reaction products were separated on denaturing 16% polyacrylamide gels followed by quantitation of DNA reaction products by phosphorimager analysis (Storm 860; Molecular Dynamics/Image Quant version 5.1 software). Fitting the Michaelis−Menten equation to velocity versus substrate concentration derived kinetic constants K_m and V_{max}. The results of two to four independent determinations were averaged. Results were analyzed statistically using a two-tailed unpaired *t*-test (Welch's *t*-test).

Translesion Synthesis Reactions of m6G-Containing Templates. Polymerase reactions were performed as described above. Each reaction contained 5 pmol of primer-template hybrid and 100, 150, or 95 pmol of WT, R253M, and E249K pol β, respectively, to analyze complete TLS opposite the m6G lesion. To assay extension of m6G-containing terminal base pairs, reactions contained 10, 20, or 10 pmol of WT, R253M, and E249K pol β, respectively. The increased amounts of polymerase for the translesion synthesis assays reflect the inhibitory nature of the template modification since reactions with lower concentrations of enzyme resulted in no primer extension (data not shown). Reaction products were separated and quantitated as above. The percentage of DNA synthesis (percent of total) at each template position in the gap-filling reaction for each polymerase reaction was quantitated as the amount of extended primer molecules of a given length divided by the total amount of primer molecules. Reactions were performed in duplicate. Differences in the distribution of TLS products using G or m6G templates were analyzed using a Kruskal Wallis nonparametric ANOVA test, at a 0.05 significance level. The percent complete TLS for the m6G template lesion is the sum of all products synthesized to the site of the lesion or beyond divided by the total primer extension. By definition, the percent TLS for the lesion extension reactions is equivalent to the total primer extension. Differences in the relative percent TLS for unmodified versus modified templates were analyzed using a two-tailed unpaired *t*-test (Welch's *t*-test).

Damage-Induced HSV-tk Polymerase Error Assay. Alkylated DNA substrates were created by random DNA modi-

fication of DNA synthesis templates as previously described (*24*). The in vitro reactions for mutational analysis contained 1.8 pmol of the MNU-modified template DNA at 40 nM concentration, 500 μM dNTPs, and 100, 150, or 95 pmol of pol β WT, R253M, and E249K, respectively (adjusted for equivalent activity). Reactions were incubated at 37 °C for 60 min and terminated with 15 mM EDTA. The extent of DNA synthesis was determined by parallel reactions (0.2 pmol of DNA; same molar ratios of enzyme to substrate as above) supplemented with 5 μCi of [α-^{32}P]dCTP (3000 Ci/mmol). A 64-mer oligonucleotide was 5′-labeled using [γ-^{32}P]ATP (5000 Ci/mmol) and T4 polynucleotide kinase, and 50 fmol was added to each reaction after termination for use as an internal loading standard. The DNA products were analyzed on an 8% polyacrylamide gel together with a DNA sequencing ladder generated from the same primer-template pair, followed by phosphorimager analysis. The amount of synthesis in each reaction was normalized to the internal standard.

Mutational analyses of the reaction products were performed after isolation and hybridization of DNA synthesis products to a gapped heteroduplex molecule, as reported previously (*24*). Hybridized gapped duplex molecules were used to electroporate *recA13, upp, tdk E. coli* strain FT334, and herpes simplex virus−*thymidine kinase* (HSV-*tk*) mutant plasmids were selected by growth on defined media containing 40 μM 5-fluoro-2′-deoxyuridine (FUdR) and 50 μg/mL chloramphenicol (Cm) as described (*24*). The HSV-*tk* mutant frequency is defined as the number of colonies resistant to both FUdR and Cm divided by the total number of Cm-resistant colonies (*24*). DNA sequence changes of independent FT334 mutants were determined and mutational spectra derived, as described (*24*). The MNU DNA modification followed by the HSV-*tk* forward mutation assay was repeated five independent times. Mutation frequency results were analyzed statistically using a nonparametric Spearmanns correlation analysis and Wilcox ranks sum test, at a 0.05 level of significance.

RESULTS

Modified Nucleotide Insertion by Variant and WT Polymerases. We used a steady-state primer extension assay with gapped DNA templates to determine whether pol β residues Arg-253 and Glu-249 are involved in discrimination of dNTPs modified at either the sugar or the base moiety. Previous studies of pol β have analyzed amino acid residues in the active site (such as Arg-283) which, when mutated, exhibit a large (>1000-fold) difference in kinetic parameters along with a severe loss of catalytic activity. In contrast, both of the variant polymerases used in this study show robust catalytic activity. Consistent with their efficient catalysis, previous kinetic results show relatively smaller differences in kinetic parameters (*6*, *7*). We have confirmed the previous results for AZT-TP discrimination by R253M using a five-nucleotide gapped DNA template. WT pol β strongly discriminates against incorporation of AZT-TP, as the inherent reactivity (V_{max}/K_m) ratio of the modified substrate relative to the natural substrate (discrimination factor) is 85 (Table 1). The variant R253M displays an enhanced discrimination against AZT-TP, relative to WT polymerase, as the discrimination factor for the variant is 210 (Table 1). These discrimination values are very similar to the inherent reactivity ratio values previously reported for WT pol β and R253M using a primed oligonucleotide template (*6*). Importantly, this level of AZT-TP discrimination observed in vitro was sufficient to impart an AZT-resistant phenotype in vivo (*6*). We extended the biochemical analyses to examine discrimination of another modification of the sugar moiety, namely, ribose versus deoxyribose. As seen in Table 1, WT pol β is somewhat more efficient at incorporating rCTP than AZT-TP, as the steady-state discrimination factor for rCTP/dCTP is 22. Again, however, the R253M variant displayed increased discrimination against the modified substrate, as the rCTP/dCTP discrimination factor for this variant was 41, 2-fold greater than WT pol β.

Table 1: Steady-State Kinetic Analyses of Modified Substrate Incorporation by Pol β WT, R253M, and E249K

enzyme	template-substrate	V_{max} (s^{-1})[a]	K_m (μM)[a]	$[V_{max}]/K_m$ ($s\cdot\mu M$)	discrimination factor[b]
β WT	A·dTTP	0.41	15	0.028	
	A·AZT-TP	0.07	232	3.3×10^{-4}	85
R253M	A·dTTP	0.34	60.3	0.0057	
	A·AZT-TP[c]	0.013	504	2.7×10^{-5}	210
β WT	G·dCTP	2.2 ± 0.6	28.6 ± 3.1	0.077	
	G·rCTP	0.6 ± 0.1	171 ± 66	0.0035	22
R253M	G·dCTP	2.8 ± 0.1	40.2 ± 2.6	0.070	
	G·rCTP	0.9 ± 0.09	516 ± 11	0.0017	41
β WT	C·dGTP	0.73 ± 0.06	10.3 ± 5.2	0.071	
	C·dm6GTP	0.14 ± 0.04	12.1 ± 5.4	0.012	5.9
R253M	C·dGTP	0.68 ± 0.06	7.9 ± 4.3	0.086	
	C·dm6GTP	0.19 ± 0.11	24.4 ± 6.7	0.0078	11[d]
E249K	C·dGTP	0.71 ± 0.05	6.6 ± 3.5	0.108	
	C·dm6GTP	0.21 ± 0.10	18.0 ± 9.1	0.012	9[d]

[a] Mean of two or average of three to four independent trials with standard deviation calculated from raw data. [b] $[V_{max}/K_m]$(natural substrate)/$[V_{max}/K_m]$(modified substrate). [c] Single determination. [d] Statistically significant relative to the corresponding WT (Welch's two-tailed unpaired *t*-test).

To examine whether this enhanced discrimination extended to dNTP modifications at the base moiety, experiments were performed using either dGTP (natural) or m6dGTP (base-modified) substrates (Figure 2). We determined the steady-state constants for dGTP and m6dGTP by WT and both the R253M and the E249K variant enzymes (Table 1). The pol β enzyme has a 5-fold higher V_{max} value for incorporation of natural dGTP (0.73 ± 0.06 s^{-1}) as compared to m6GTP (0.14 ± 0.04 s^{-1}). The K_m for incorporation by WT pol β is similar for natural dGTP (10.3 ± 0.2 μM) and m6dGTP (12.1 ± 5.4 μM). Therefore, unlike the sugar-modified nucleotides, m6GTP is a good substrate for WT pol β, as seen by the low V_{max}/K_m discrimination factor (5.9) (Table 1). Nevertheless, in agreement with the sugar-modified substrate results, the variants displayed enhanced discrimination against the m6GTP substrate. For both variants, the K_m values for m6GTP were 3-fold higher than those of dGTP. Therefore, the discrimination factor with respect to K_m ($[K_m]_{C\cdot G}/[K_m]_{C\cdot m6G}$) for the variants ($0.3 \pm 0.2$ and 0.4 ± 0.1 for R253M and E249K, respectively) differs from that for WT (1.0 ± 0.2), a difference that is statistically significant ($p = 0.0071$ and $p = 0.004$ for R253M and E249K, respectively; Welch's *t*-test). The discrimination factor with respect to V_{max} ($[V_{max}]_{C\cdot G}/[V_{max}]_{C\cdot m6G}$) for both variants ($3.6 \pm 2.0$ and 4.6 ± 2.3 for R253M and E249K, respectively) is similar to WT pol β

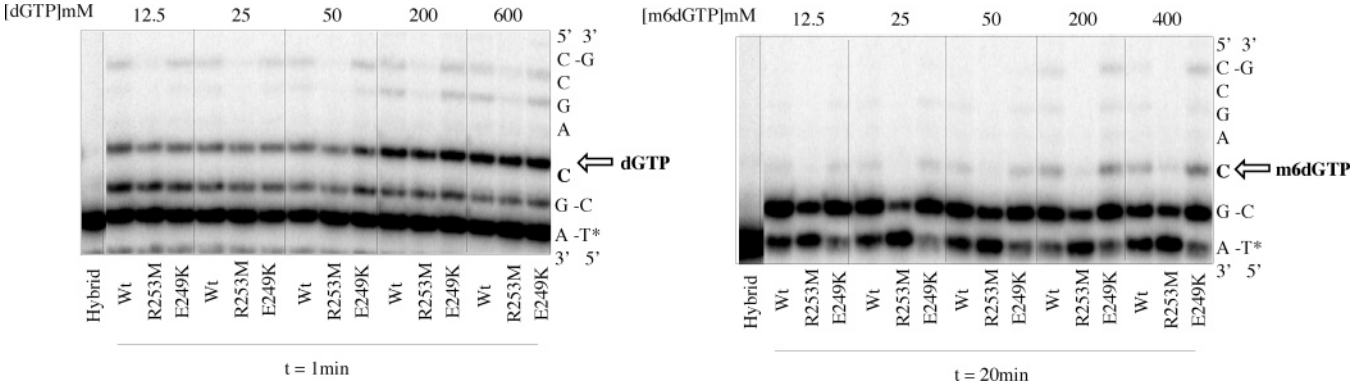

FIGURE 2: dGTP or m6dGTP incorporation for DNA pol β WT, variant R253M, and variant E249K. Representative gels for the 5′-^{32}P-labeled incorporation studies with dGTP at $t = 1$ min (left) and m6dGTP at $t = 20$ min (right) opposite template C with the following three pol β enzymes: WT and variants R253M and E249K as indicated. An asterisk denotes the 5′-labeled primer. Reactions were conducted in the presence of 50 μM dCTP (running start) and varying amounts of dGTP or m6dGTP as indicated. Since only two nucleotides were available (the running start dCTP and either dGTP or m6dGTP) for these reactions, complete gap filling required both misinsertion and mispair extension opposite template A at position +3. The amount of synthesis was quantitated by phosphorimager analysis. Kinetic values (Table 1) were calculated as discussed in Materials and Methods.

(5.9 ± 2.0). Importantly, the R253M variant retains for this base-modified dNTP substrate the 2-fold enhanced discrimination, relative to WT, at the level of inherent reactivity that was observed for the sugar-modified nucleotides (Table 1). These data support a role for Arg-253 and Glu-249 in m6dGTP discrimination and demonstrate that the major biochemical change is in the Michaelis constant term.

We next determined whether these variants play a role in discrimination of base-modified template residues. To this end, we performed translesion synthesis assays to quantitate the effect of the pol β variants, R253M and E249K, using both specific template m6G-containing and random MNU-treated templates.

Translesion Synthesis Opposite Template G and m6G Bases by Variant and WT Polymerases. We created two gapped substrates for pol β synthesis, complementary to those used above, which contained either a natural G or a modified m6G at template position +2 (Figure 1B). To examine the complete TLS, polymerase reactions were performed using both DNA hybrids and either 50 μM each dATP + dCTP (correct) or 50 μM each dATP + TTP (incorrect) substrates (Figure 3 and data not shown). The percentage of DNA synthesis for each polymerase reaction was quantitated at each template position as the amount of extended primer molecules divided by the total amount of primer molecules.

Using unmodified templates, DNA pol β WT efficiently inserts dCTP opposite G and continues DNA synthesis for two template positions (data not shown). Pol β WT displayed a lower efficiency of TTP misinsertion opposite G, consistent with previous observations (*17*). Pol β variants R253M and E249K exhibit statistically similar termination insertion patterns, relative to WT, during gap filling of unmodified templates (data not shown). When total synthesis opposite template G was quantiated relative to WT pol β, the R253M polymerase displayed a slight antimutator tendency for G·dTTP misinsertion events, while the E249K variant displayed a mutator tendency for G·dTTP misinsertions (Table 2). Although the difference observed for the E249K variant was statistically significant relative to G·dCTP insertion ($p = 0.049$), the difference for R253M was not.

Comparison of m6G TLS using either dCTP or TTP substrates by pol β WT (Figure 3A) demonstrates the preferential insertion of TTP opposite m6G, consistent with previous results for pol β WT (*17*). The distribution of insertion products opposite the m6G lesion did not differ statistically for pol β variants R253M and E249K relative to WT (Figure 3B,C). When total m6G TLS was quantitated relative to WT pol β, the R253M polymerase displayed the same antimutator tendency for m6G·dTTP misinsertion events that was observed for G·dTTP insertion (Table 2), but again, this difference was not statistically significant. The E249K variant displayed no bias for dTTP or dCTP misinsertion opposite m6G (Table 2). These data suggest that loop residues Arg-253 and Glu-249 are not involved in complete TLS past m6G-template lesions.

Nucleotide Extension of m6G-Containing Terminal Base Pairs by Variant and WT Polymerases. Complete TLS requires that a polymerase extend a lesion-containing terminal base pair. To examine this step specifically, gapped templates were designed so that the priming oligonucleotide created a correct G·C or an incorrect G·T base pair and either a nonmutagenic m6G·C or mutagenic m6G·T base pair at the primer terminus (Figure 1C). Under nonlimiting enzyme conditions, pol β WT efficiently extends both the G·C and G·T primer termini, and no significant differences in G·T extension by pol β variants R253M and E249K were observed, relative to WT (Table 2). Pol β WT displayed efficient extension of a m6G·C primer terminus (Figure 4A,C), consistent with previous observations (*17*). Pol β WT extended an m6G·T primer terminus less efficiently than the m6G·C template (Figure 4B,D). We observed no statistically significant difference between the distribution of extension products for pol β variant R253M and E249K using m6G·C and m6G·T termini relative to WT (Figure 4C,D). When total extension products from m6G·T and m6G·C were quantitated, no significant differences between WT pol β and either variant were observed (Table 2). These data suggest that residues Arg-253 and Glu-249 are not involved in extension of m6G-containing terminal base pairs.

Response of WT and Variant Pol β to Random MNU Alkylation. The in vitro HSV-*tk* forward mutation assay was used to determine whether variants R253M and E249K display altered discrimination of base lesions induced by random MNU template alkylation. In side-by-side experi-

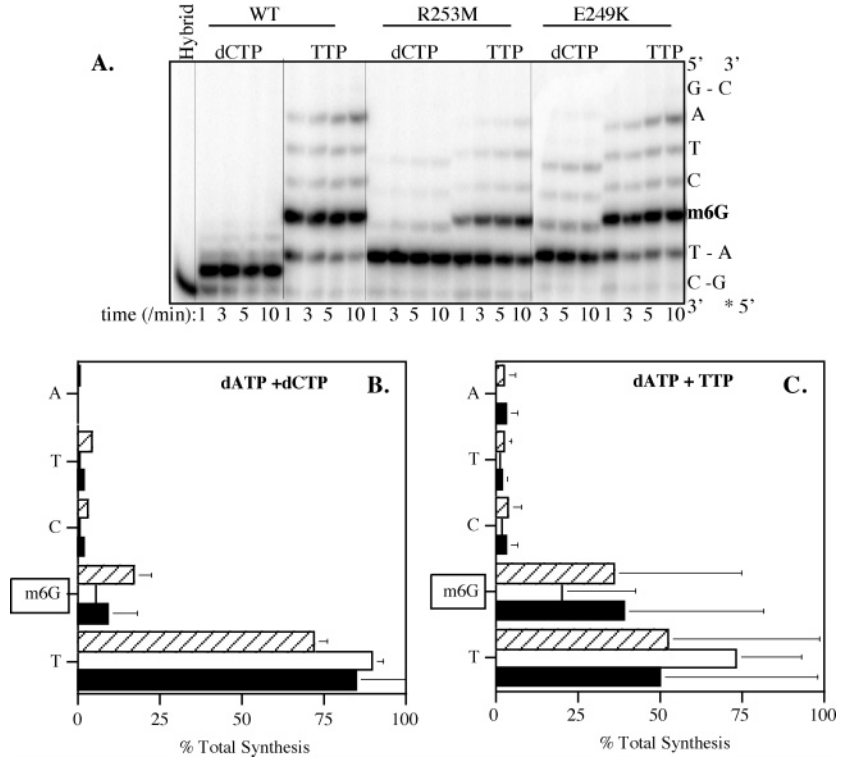

FIGURE 3: Complete translesion synthesis opposite the m6G-containing template by DNA pol β WT and variants R253M and E249K. (A) Representative gel showing extension of the m6G-containing template, hybrid 3. An asterisk denotes the 5′-labeled primer. Reactions were conducted in the presence of 50 μM dATP (running start) and 50 μM dCTP or TTP as indicated and quenched at 1, 3, 5, and 10 min intervals. Reaction products were separated by denaturing gel electrophoresis. (B, C) Quantitation of m6G translesion synthesis by DNA pol β WT (black bars), R253M (open bars), and E249K (hatched bars). Reaction products were quantitated by phosphorimager analysis of 3 min reactions performed in the presence of dCTP (B) or TTP (C). The percent total synthesis was determined at the specified template position (*y*-axis) within the gapped template. Data are the mean (standard deviation) of two independent experiments.

Table 2: Translesion Synthesis by R253M and E249K Variants Relative to Pol β WT

	template % TLS (relative to WT pol β)[a]: complete			
pol β form	G·dCTP	G·dTTP	m6G·dCTP	m6G·dTTP
R253M	1.00 ± 0.05	0.54 ± 0.19	0.80 ± 0.63	0.52 ± 0.04
E249K	1.02 ± 0.06	1.58 ± 0.02	3.4 ± 0.69	1.46 ± 0.66
	template % TLS (relative to WT pol β)[a]: extension			
pol β form	G·C	G·T	m6G·C	m6G·T
R253M	0.77 ± 0.03	0.96 ± 0.01	0.82 ± 0.24	0.55 ± 0.19
E249K	1.19 ± 0.05	1.05 ± 0.02	0.99 ± 0.00	1.48 ± 0.17

[a] Data were calculated from TLS reactions such as those shown in Figures 3 (complete) and 4 (extension). Primary data for the unmodified templates are not shown. Percentage TLS relative to WT values are the mean ± standard deviation of two trials.

ments, all three polymerases displayed similar DNA synthesis inhibition with increasing MNU concentration (Figure 5A). Using solvent-treated templates, the HSV-*tk* forward mutation frequency for WT pol β was (120 ± 50) × 10^{-4}, similar to that previously reported using 1 mM dNTP (*25*). For the WT polymerase, we observed a linear mutational dose response up to 10 mM MNU, and a 10-fold increased mutational frequency [(1200 ± 410) × 10^{-4}], relative to solvent control (Figure 5B). At the 10 mM dose, the mean mutation frequency measured for variant R253M was (700 ± 154) × 10^{-4}, a 9-fold increase relative to solvent control, while variant E249K was (1300 ± 830) × 10^{-4}, an 8-fold increase relative to solvent control. The MNU mutation rates, defined by the slope of the mutation versus dose response curve, for pol β WT compared with variants R253M and E249K do not show a statistically significant difference.

To examine whether the variants produced the same errors as WT pol β, we generated mutational spectra from DMSO (solvent only) and MNU-treated template for each enzyme. The solvent control polymerase error frequencies reflect the antimutator tendency of R253M and mutator tendency of E249K previously observed (*6*). Specifically, pol β variant E249K produced elevated levels of both G → A (involving G·TTP mispair) transitions (3.2-fold) and G → T (G·dATP mispair) transversions relative to pol β WT (Figure 6). Although no G → T transversion mutations were produced by the wild-type enzyme in this study, we previously observed a single G → T transversion by pol β for a mutation frequency of ∼1 × 10^{-4} (*25*). Therefore, the magnitude of the E249K mutator effect for this specific error is ∼30-fold on solvent-treated templates. The control frequency of G → A base substitutions was 2.2-fold lower for R253M than WT (Figure 6).

As expected due to m6G lesions, 10 mM MNU treatment of template DNA resulted in an approximately 20-fold increased frequency of G → A transitions (160 × 10^{-4}), relative to solvent control (7.4 × 10^{-4}) produced by pol β WT (Figure 6). The distribution of G → A transitions did not vary between WT and variant pol β enzymes (Figure 7). The MNU-induced G → A transition frequency was not different among the three polymerase forms at any MNU dose from 5 to 20 mM (Figure 6 and data not shown). This observation is consistent with the lack of an effect of the loop domain variants on m6G TLS in the biochemical assays.

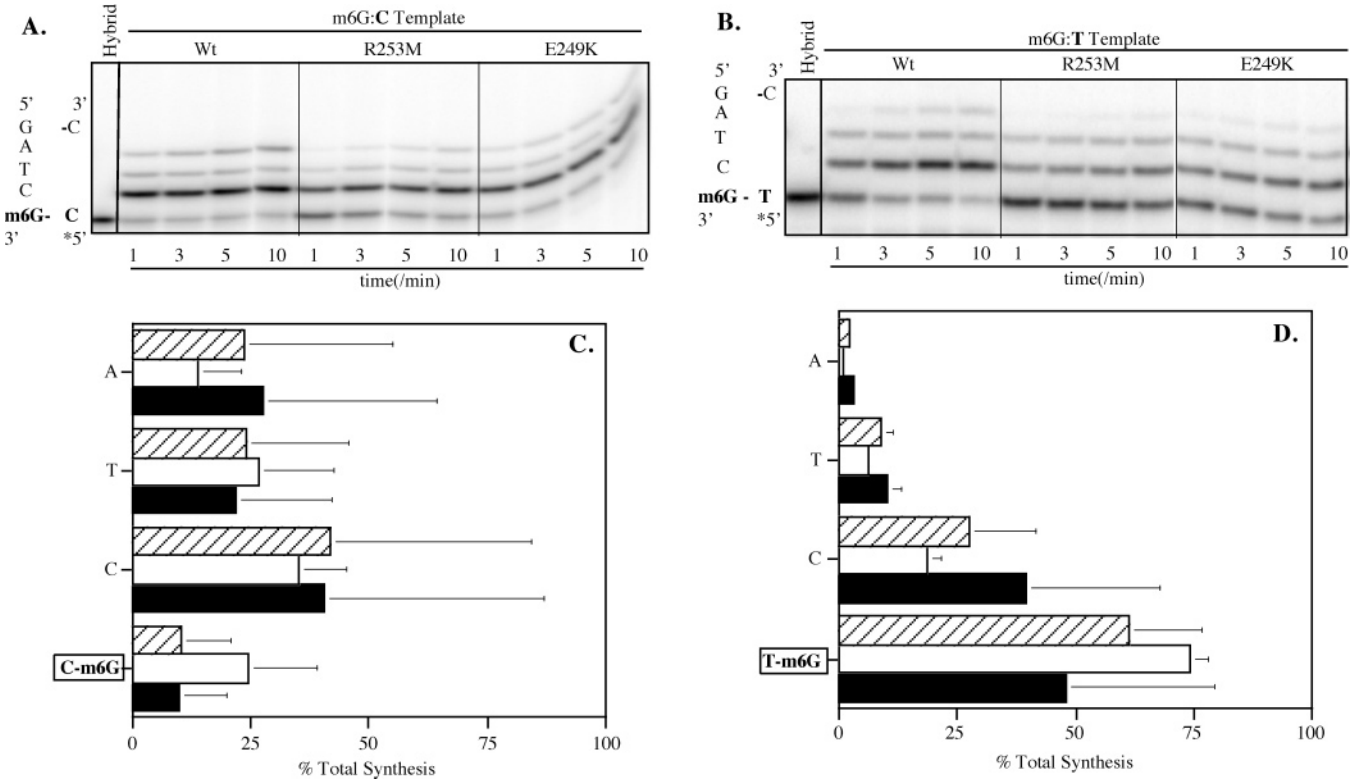

FIGURE 4: Translesion extension synthesis by DNA pol β WT and variants R253M and E249K at m6G·C and m6G·T termini. Representative gels showing reaction products for extension of (A) m6G·C termini (hybrid 3) and (B) m6G·T termini (hybrid 6) in the presence of 50 μM dGTP as a function of time (1−10 min). An asterisk denotes the 5′-labeled primer. (C, D) Quantitation of extension synthesis by DNA pol β WT (black bars), R253M (open bars), and E249K (hatched bars). Reaction products such as those represented in (A) and (B) were quantitated by phosphorimager analysis of 3 min reactions. The percent total nucleotide extended past the specified template position (*y*-axis) is shown for m6G·C (C) and m6G·T (D) substrates. The results are the mean (standard deviation) of two independent trials.

However, MNU treatment also resulted in a large increase in the frequency of C → A transversions produced by WT pol β (90×10^{-4}), relative to solvent controls ($\leq 3.7 \times 10^{-4}$). Interestingly, this class of alkylation-induced errors was observed to vary by polymerase, and the frequency of MNU-induced C → A transversions was 3-fold higher for E249K (270×10^{-4}) and 2-fold lower for R253M (43×10^{-4}), relative to WT (Figure 6).

DISCUSSION

The DNA pol β variants R253M and E249K reside within a disordered loop of the palm subdomain and were originally identified in a genetic screen for AZT resistance (*6*). R253M displays reduced steady-state misincorporation of AZT-TP in vitro (*6*) (Table 1), while pol β variant E249K displays an altered kinetic mechanism of dNTP discrimination and an increased ability to extend template·dNTP mispairs (*7*). We have extended the characterization of these variants by examining their discrimination of other nucleotide modifications. We observed an enhanced discrimination by R253M for rCTP versus dCTP substrates and enhanced discrimination of m6GTP versus dGTP substrates by both R253M and E249K (Table 1). We observed a statistically significant 3-fold decreased K_m ratio of m6dGTP/dGTP for pol β variants R253M and E249K, relative to WT (Table 1). However, we observed no significant difference in V_{max} discrimination of m6dGTP between variants and WT. Overall, a small, but consistent, enhanced substrate discrimination by R253M, relative to WT, was observed for three distinct modifications of both purine and pyrimidine nucleotides: 3′-ribose (AZT-TP vs TTP), 2′-ribose (rCTP vs dCTP), and base (m6dGTP vs dGTP). The observed 2-fold difference in AZT-TP discrimination between the R253M variant and WT pol β was previously shown to be sufficient to confer an AZT-resistant phenotype in vivo (*6*).

Several models have been proposed previously for how the loop domain variants affect nucleotide discrimination. The loop may directly interact with nucleotide substrates, perhaps by channeling the dNTPs into the active site (*7*). Alternatively, the loop is a structural component of the catalytic palm subdomain and, as such, may function to maintain optimal active site geometry. Finally, the flexible loop may function indirectly in nucleotide discrimination by modulating the DNA primer position within the pol β active site (*8*). We investigated whether the R253M and E249K variants affect discrimination of alkylated DNA template lesions. For this study, we focused on the m6G base modification, as many studies have examined the structural basis of m6G mutagenesis. Physical structures have demonstrated that the m6G·T base pair assumes a Watson−Crick-like conformation while the m6G·C base pair is primarily in a wobble conformation (*13*). Kinetic and biochemical studies have demonstrated that minor groove interactions between the polymerase and the m6G-containing DNA template are critical for efficient translesion synthesis by the Klenow polymerase (*19*, *20*). Minor groove recognition by DNA polymerases depends on the correct positioning of the DNA substrates and key amino acid residues within the catalytically competent closed conformation. The slow rate of incorporation opposite m6G by the Klenow poly-

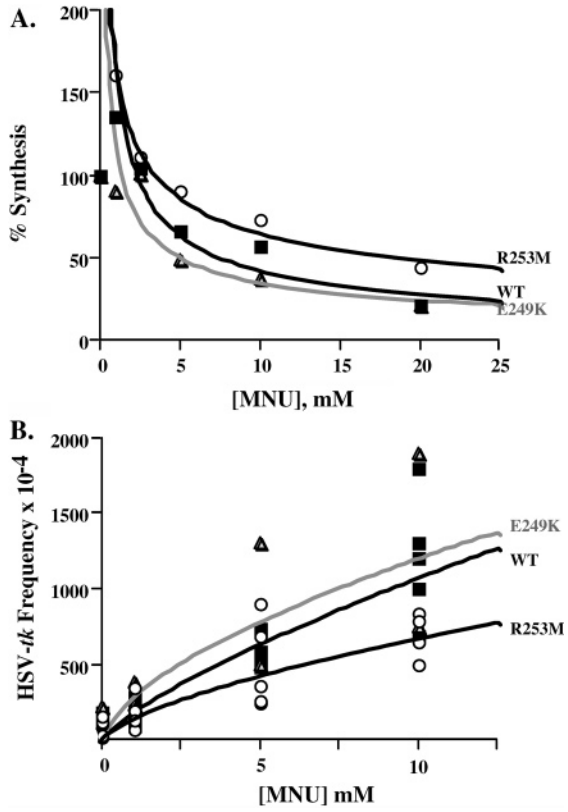

FIGURE 5: DNA synthesis inhibition and mutagenesis in response to random MNU alkylation of template DNA for DNA pol β WT (black square), variant R253M (open circle), and variant E249K (gray triangle). (A) Results for the percent synthesis on MNU-treated single-strand DNA. The amount of synthesis was quantitated by PAGE separation and phosphorimager analysis (Materials and Methods). The data shown are percent of solvent control. (B) Mutational response to MNU-treated template. The HSV-*tk* mutation frequency was determined by transfection of reaction products and selective plating (Materials and Methods).

merase has been attributed to unfavorable alignment of 3′OH for in-line attack of the incoming dNTP due to altered structure of the lesion base pair (*15*).

If the altered fidelity displayed by variants R253M and E249K is due to distorted active site geometry, then we hypothesized that both enzymes would display enhanced discrimination against the m6G template modification due to structural changes caused by the m6G base pairing during active site assembly. However, the results of our biochemical assays indicate that R253M and E249K variants fail to exhibit altered discrimination of m6G-modified template lesions, contrary to what was observed for discrimination of the m6GTP nucleotide substrate. This conclusion was also reached after examining mutations induced by WT and variant pol β enzyme during replication of MNU-alkylated DNA templates. The frequency and distribution of methylation-induced G → A transition mutations were similar for all three polymerases (Figures 6 and 7). Together, the biochemical and genetic results suggest that residues Arg-253 and Glu-249 do not play a significant role in recognizing m6G-modified template residues, although both variants show a difference in m6G-modified dNTP discrimination.

We confirmed the altered fidelity previously reported for R253M (*6*) and E249K (*7*) by mutational analyses of polymerase-induced errors using solvent control templates. R253M consistently showed a lower mutation frequency

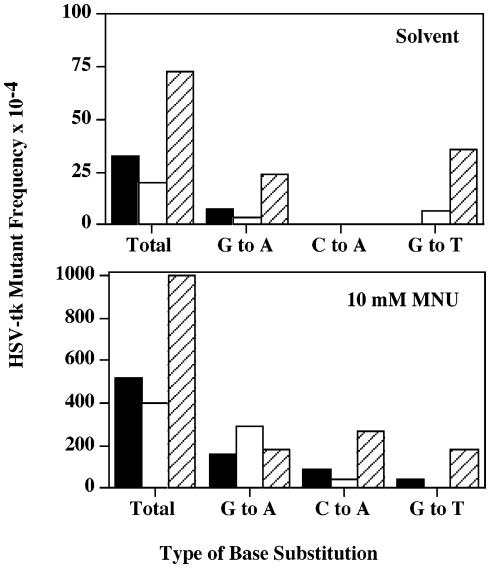

FIGURE 6: Mutational specificity of variants and wild-type pol β using solvent and MNU-modified DNA templates. Products of DNA synthesis reactions were introduced into *E. coli*, and independent HSV-*tk* mutants were selected and analyzed for DNA sequence changes. Key: solid bars, wild-type pol β; open bars, R253M; hatched bars, E249K. The absolute solvent-induced mutation frequencies and number of mutants sequenced were as follows: wild-type pol β, 140×10^{-4} ($N = 38$); R253M, 120×10^{-4} ($N = 36$); E249K, 220×10^{-4} ($N = 18$). The absolute 10 mM MNU-induced mutation frequencies were as follows: wild-type pol β, 1100×10^{-4} ($N = 49$); R253M, 720×10^{-4} ($N = 50$); E249K, 1900×10^{-4} ($N = 41$).

compared to WT pol β, consistent with an antimutator tendency (Figures 5 and 6). In contrast, E249K has a mutator phenotype, and we observed an increased base substitution mutation frequency for the variant (Figure 6). We note that E249K displayed an increase in G·dTTP insertion and an increase in the frequency of G → A transitions on control templates, relative to WT pol β. Random methylation of the ssDNA template induced a ≥20-fold increased frequency of WT pol β-induced C → A transversion mutations (Figure 6). We have previously observed these alkylation-induced transversions using MNU-treated templates and exonuclease-deficient T4 polymerase (*26*) as well as *N*-ethyl-*N*-nitrosourea-treated ssDNA templates and WT pol β (*25*). The mutational mechanism for C^{alk} → A errors is not known but is assumed to be due to dTTP misincorporation opposite either O^2-alkylcytosine or N3-alkylcytosine, the latter of which is formed at significant levels by alkylation of ssDNA. In this study, we observed a mutator phenotype for alkylation-induced C → A transversion errors for the E249K polymerase, consistent with the increased efficiency of C·TTP mispair extension relative to wild type previous reported (*7*). In summary, the mutational specificity analysis demonstrates that the E249K variant is a mutator polymerase and the R253M is an antimutator polymerase and that the mutator/antimutator phenotypes are displayed for only a subset of alkylation-induced errors.

Our lesion discrimination results support either of two mechanisms for the involvement of the flexible loop in pol β fidelity: a direct effect on recognition or interaction with the incoming dNTP (*7*) or an indirect effect on positioning of the DNA primer within the active site (*8*). Our results do not support the model wherein the loop affects active site geometry (*7*), as we failed to observe differences between

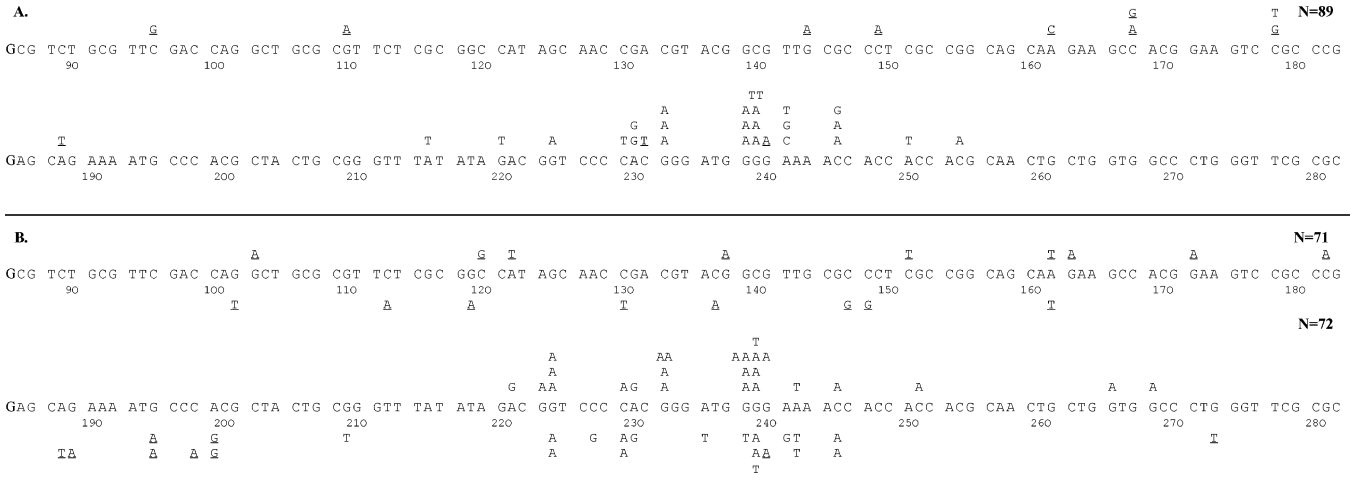

FIGURE 7: Partial mutational spectra for 5 and 10 mM MNU-treated templates. (A) Base substitution errors produced by pol β WT. (B) Base substitution errors produced by pol β variants R253M (above) and E249K (below). *N* indicates the total number of mutants sequenced for each group, and an underline indicates sequence changes detected as part of a multiple mutation.

the loop variants and WT pol β in m6G template discrimination. Arg-253 and Glu-249 form part of a flexible three-dimensional loop region that may interact with dNTPs prior to base pairing and catalysis. On the basis of their structural studies of the Klenow fragment of Taq polymerase, Li et al. proposed that dNTP substrates may be delivered to the active site by binding to helix O, followed by a conformational change of the fingers region. In this way, polymerases may be able to sample all four dNTPs in a fast process by delivering them to the active site; however, only the correct dNTP will lock the enzyme in the closed, catalytically competent ternary complex (*27*). Evidence for dNTP substrate binding along the O helix in the open conformation with primer-template DNA has been reported by others (*28*). We have observed that the R253M and E249K loop variants display altered discrimination of nucleotides modified at both the sugar and base moieties (Table 1). Perhaps specific interactions of the incoming dNTP with the loop region are required for substrate channeling or delivery to the pol β active site, and these interactions are disrupted in the variants. In this model, the observed changes in fidelity, which are specific for a subset of base substitution errors, may be caused by altered delivery of dNTP substrates.

Alternatively, our data for lesion discrimination by the loop variants could be explained by a mechanism wherein the flexible loop helps to correctly position the DNA primer within the catalytically competent ternary complex. Translesion synthesis of methylated C lesions by the loop variants is altered in a manner predicted from the fidelity of the variants on undamaged DNA templates (e.g., a mutator tendency for E249K and an antimutator tendency for R253M). The O^2 position of cytosine is one site of minor groove recognition via hydrogen bonding between the polymerase and the DNA. If the premutagenic lesion for the alkylation-induced C $\rightarrow$ A transversion errors in O^2-methyl-C, then polymerase fidelity would be expected to be compromised due to loss of this DNA substrate interaction. Regardless of the precise chemical nature of the premutagenic lesion, the C $\rightarrow$ A transversions require formation and extension of a pyrimidine−pyrimidine mispair, which is also expected to severely affect DNA geometry and positioning within the active site (*12*). The effect of pol β loop variants on this specific class of alkylation-induced errors could potentially be due to altered positioning of the DNA primer 3′OH or the incoming dTTP within the active site in a manner that either enhances (E249K) or exacerbates (R253M) the chemistry step. In both of these models, we assume that the structural changes caused by template m6G·C and m6G·T mispairs are too subtle to be affected by the structural alterations present in either the R253M or the E249K variant.

In summary, our findings demonstrate that the loop in the palm domain of pol β, an area with an unknown function, is involved in discrimination of nucleotide substrates modified at both the base and sugar moieties. This study highlights the importance of residues distant from the active site in pol β fidelity, since single amino acid substitutions of two different residues within the flexible loop in the palm domain affect pol β nucleotide selection. While the variants can discriminate m6G modification of the dNTP, they display no altered recognition of the m6G lesion present in the template DNA. However, the variants do display altered discrimination of alkylated template C lesions. Our results support two previously proposed models for the functioning of the flexible loop in pol β fidelity. In depth, pre-steady-state kinetic analyses can be performed in future studies in order to definitively elucidate the mechanism by which the flexible loop contributes to lesion discrimination.

ACKNOWLEDGMENT

We thank Dr. Joann Sweasy (Yale University) for WT and variant pol β vector clones, Dr. Susan Dallabrida for technical assistance with DNA pol β variant R253M, and Guang Yan for the DNA sequence analyses. We also thank Suzanne Hile and Dr. Erin Gestl for critical reading of the manuscript.

REFERENCES

1. Idriss, H., Al-Assar, O., and Wilson, S. (2002) DNA Polymerase Beta, *Int. J. Biochem. Cell Biol. 34,* 321−324.
2. Plug, A., Clairmont, C., Spi, E., Ashley, T., and Sweasy, J. (1997) Evidence for the role of DNA polymerase beta in mammalian meiosis, *Proc. Natl. Acad. Sci. U.S.A. 94,* 1327−1331.
3. DiGiuseppe, J., and Dresler, S. (1989) Bleomycin-induced DNA repair synthesis in permeable human fibroblasts: mediation of long-patch and short-patch repair by distinct DNA polymerases, *Biochemistry 28,* 9515−9520.

4. Narayan, S., Beard, W., and Wilson, S. (1995) DNA damage-induced transcriptional activation of a human DNA polymerase beta chimeric promoter: recruitment of preinitiation complex, *Biochemistry 34*, 73−80.
5. Sweasy, J. (2003) Fidelity mechanisms of DNA polymerase beta, *Prog. Nucleic Acid Res. 73*, 137−169.
6. Kosa, J., and Sweasy, J. (1999) 3′-Azido-3′-deoxythymidine-resistant mutants of DNA polymerase beta identified by in vitro selection, *J. Biol. Chem. 274*, 3851−3858.
7. Kosa, J., and Sweasy, J. (1999) The E249K mutator mutant of DNA polymerase beta extends mispaired termini, *J. Biol. Chem. 274*, 35866−35872.
8. Dalal, S., Kosa, J., and Sweasy, J. (2004) The D246V mutant of DNA polymerase beta misincorporates nucleotides, *J. Biol. Chem. 279*, 577−584.
9. Krahn, J., Beard, W., and Wilson, S. (2004) Structural insights into DNA polymerase beta: Deterrents for misincorporation support an induced fit mechanism for fidelity, *Structure 12*, 1823−1832.
10. Fersht, A. (1997) *Enzyme Structure and Mechanism*, 2nd ed., W. H. Freeman, New York.
11. Sawaya, M., Prasad, R., Wilson, S., Kraut, J., and Pelletier, H. (1997) Crystal Structures of DNA Polymerase Beta Complexed with Gapped and Nicked DNA: Evidence for an Induced Fit Mechanism, *Biochemistry 36*, 11205−11215.
12. Johnson, S., and Beese, L. (2004) Structures of mismatch replication errors observed in a DNA polymerase, *Cell 116*, 803−816.
13. Swann, P. (1990) Why do O^6-alkylguanine and O^4-alkylthymine miscode? The relationship between the structure of DNA containing O^6-alkylguanine and O^4-alkylthymine and the mutagenic properties of these bases, *Mutat. Res. 233*, 81−94.
14. Dosanjh, M., Loechler, E., and Singer, B. (1993) Evidence from in vitro replication that O^6-methylguanine can adopt multiple conformations, *Proc. Natl. Acad. Sci. U.S.A. 90*, 3983−3987.
15. Tan, H., Swann, P., and Chance, E. (1994) Kinetic analysis of coding properties of O^6-methylguanine in DNA: The crucial role of the conformation of the phosphodiester bond, *Biochemistry 33*, 5335−5346.
16. Reha-Kratz, L., Nonay, R., Day, R., III, and Wilson, S. (1996) Replication of O^6-methylguanine-containing DNA by repair and replicative DNA polymerases, *J. Biol. Chem. 271*, 20088−20095.
17. Singh, J., Su, L., and Snow, E. (1996) Replication across O^6-methylguanine by human DNA polymerase beta in vitro, *J. Biol. Chem. 271*, 28391−28398.
18. Dosanjh, M., Galeros, G., Goodman, M., and Singer, B. (1991) Kinetics of extension of O^6-methylguanine paired with cytosine or thymine in defined oligonucleotide sequences, *Biochemistry 30*, 11595−11599.
19. Spratt, T. (1997) Klenow fragment-DNA insertion required for the incorporation of nucleotides opposite guanine and O^6-methylguanine, *Biochemistry 39*, 13279−13297.
20. Gestl, E. E., and Eckert, K. A. (2005) Loss of DNA minor groove interactions by exonuclease-deficient Klenow polymerase inhibits O^6-methylguanine and abasic site translesion synthesis, *Biochemistry* (in press).
21. Kunkel, T., and Wilson, S. (1998) DNA polymerases on the move, *Nat. Struct. Biol. 5*, 95−99.
22. Morales, J., and Kool, E. (2000) Functional hydrogen-bond map of the minor groove binding tracks of six DNA polymerases, *Biochemistry 39*, 12979−12988.
23. Opresko, P., Shiman, R., and Eckert, K. (2000) Hydrophobic interactions in the hinge domain of DNA polymerase beta are important but not sufficient for maintaining fidelity of DNA synthesis, *Biochemistry 39*, 11399−11407.
24. Eckert, K., Hile, S., and Vargo, P. (1997) Development and use of an in vitro HSV-tk forward mutation assay to study eukaryotic DNA polymerase processing of DNA alkyl lesions, *Nucleic Acids Res. 25*, 1450−1457.
25. Eckert, K., and Hile, S. (1998) Alkylation-induced frameshift mutagenesis during in vitro DNA synthesis by polymerase alpha and beta, *Mutat. Res. 422*, 255−269.
26. Khare, V., and E., K. (2001) The 3′-5′ exonuclease of T4 DNA polymerase removes premutagenic alkyl mispairs and contributes to futile cycling at O^6-methylguanine lesions, *J. Biol. Chem. 276*, 24286−24292.
27. Li, Y., Korolev, S., and Wakesman, G. (1998) Crystal structures of open and closed forms of binary and ternary complexes of the large fragment of *Thermus aquaticus* DNA polymerase I: structural basis for nucleotide incorporation, *EMBO J. 17*, 7514−7525.
28. Johnson, S., Taylor, J., and Beese, L. (2003) Processive DNA synthesis observed in a polymerase crystal suggests a mechanism for the prevention of frameshift mutations, *Proc. Natl. Acad. Sci. U.S.A. 100*, 3895−3900.

BI047444I